J. Fluid Mech. (1969), *vol.* 38, *part* 2, *pp.* 401–414
Printed in Great Britain

Non-linear theory of unstable plane Poiseuille flow

By E. H. DOWELL
Princeton University

(Received 7 November 1968 and in revised form 6 January 1969)

A theoretical study of plane Poiseuille flow is made using the full non-linear Navier–Stokes equations. The mathematical technique employed is to use a Fourier decomposition in the streamwise spatial variable, a Galerkin expansion in the lateral variable and numerical integration with respect to time. By retaining the non-linear terms, the limit cycle oscillations of an unstable (in a linear sense) flow are obtained. A brief investigation of the possibility of instability due to large (non-linear) disturbances is also made. The results are negative for the cases examined. Comparisons with results previously obtained by others from linear theory illustrate the accuracy and efficacy of the method.

1. Introduction

In recent years there has been considerable interest in treating the non-linear behaviour of viscous flows which are unstable in the linear approximation. Such studies appear to be the most rational way of approaching 'turbulence', which may be considered to be the non-linear oscillations of an unstable laminar flow. Notable contributions have been made by Stuart (1960), Watson (1960) and Eckhaus (1965). Stuart and Watson used what may be termed in the present context a one-mode approximation while Eckhaus formally considered multi-mode expansions in terms of the eigenfunctions of the linear problem. Because usually only the first eigenfunction is available at considerable effort (see, for example, Lin (1955)), such multi-mode expansions are not directly useful for quantitative analysis. In the present paper the Galerkin method using a primitive model expansion is employed for plane Poiseuille flow. These primitive modes satisfy the boundary conditions of the problem but not the eigenfunction equation. They are chosen *a priori* for their simplicity in mathematical manipulation. The analysis is carried through to the point of obtaining interesting analytical and numerical results. Galerkin's method has been widely used in many physical contexts for non-linear oscillations and also for linear problems in viscous flow, see Gallagher & Mercer (1962).

An alternate and popular technique is the method of finite differences. Thomas (1953) pioneered its use for the linear problem. Most recently Dixon & Hellums (1967) have considered the non-linear problem using finite differences. While some criticism of details of their analysis may be made, they have shown the basic feasibility of such a method. Generally speaking, however, Galerkin's method is to be preferred (for simple flow geometries) because the choice of the modal expansion is at the disposal of the investigator. A suitable choice of modes based upon some insight into the physical nature of the problem will often permit analytical and numerical results to be obtained more readily than *via* a finite-difference procedure. Indeed this is the basis of the Stuart–Watson approach.

An earlier paper by Meksyn & Stuart (1951) is relevant to the present study in that it treats plane Poiseuille flow. They solve simultaneously the usual (linear) perturbation equation plus a (non-linear) mean flow equation to investigate the effect of large initial disturbances on the stability of the flow.

This approach is suitable for analytical approximation but is perhaps less systematic than that adopted here. Also it is not suitable for obtaining information about the non-linear fluid oscillations themselves which is the principal interest here.

After the present work was completed the work of Grosch & Salwan (1968) became available wherein the *linear* problem is treated by a method similar to that employed here. They also drew attention to the earlier work by Dolph & Lewis (1958), who treated the linear problem and anticipated the usefulness of the modal expansion (Galerkin) approach for the non-linear problem.

2. Problem formulation

The equation of motion for a two-dimensional, incompressible viscous flow in terms of a perturbation stream function is

$$\frac{\nabla^4\psi}{R}-\frac{\partial}{\partial t}(\nabla^2\psi)-\overline{u}\frac{\partial}{\partial x}\nabla^2\psi+\frac{d^2\overline{u}}{\partial y^2}\frac{\partial\psi}{\partial x}=\frac{\partial\psi}{\partial y}\frac{\partial}{\partial x}\nabla^2\psi-\frac{\partial\psi}{\partial x}\frac{\partial}{\partial y}\nabla^2\psi. \tag{2.1}$$

The velocity components are given by

$$u_T=\overline{u}+u=\overline{u}+\frac{\partial\psi}{\partial y},$$

and

$$v_T=v=-\frac{\partial\psi}{\partial x}. \tag{2.2}$$

The mean steady velocity profile, $\overline{u}$, whose stability we examine, is given by

$$\overline{u}=y-y^2; \tag{2.3}$$

i.e. we treat plane Poiseuille flow. The non-dimensionalization is such that y and x are normalized by channel height, h, and the velocities by four times the mid-channel mean velocity. Note that, from (2.3),

$$\overline{u}=\tfrac{1}{4}\quad\text{at}\quad y=\tfrac{1}{2}. \tag{2.4}$$

The Reynolds number is therefore

$$R\equiv\frac{Vh}{\nu},$$

where V is four times $\overline{u}$ at $y=\frac{1}{2}$ and ν the kinematic viscosity.

The boundary conditions of zero velocity at the walls require

$$\left.\begin{aligned}\partial\psi/\partial x&=0\quad\text{at}\quad y=0,1,\\ \partial\psi/\partial y&=0\quad\text{at}\quad y=0,1.\end{aligned}\right\} \tag{2.5}$$

We shall seek a solution in the form of an expansion

$$\psi(x,y,t) = \sum_{m=1}^{\infty} \sum_{v=0}^{\infty} [A_{mv} \cos v\alpha x + B_{mv} \sin v\alpha x]\, \psi_m(y), \tag{2.6}$$

where m and v run over integer values. The ψ_m will be chosen to satisfy the boundary conditions (2.5), namely

$$\psi_m(y) \equiv \cos(m-1)\pi y - \cos(m+1)\pi y. \tag{2.7}$$

These functions form a complete but not an orthogonal set; their analytical character makes such a choice convenient from the point of view of computation. The x dependence is taken to be harmonic in order that the solution remain bounded as $x \to \pm\infty$. To account for all possible interactions one should really replace the sum over v by a continuous spectrum. However, one expects the discrete harmonics to dominate since if a given single harmonic α is excited then only integer multiples of α will occur. Note further that since the non-linearity is of second order (see right-hand side of (2.1)) the dominant harmonics will probably be $v = 0$ and 2. This should be verified by computation, of course.

The Galerkin solution procedure proceeds by substituting (2.6) into (2.1) and multiplying the result by $\cos s\alpha x \psi_r(y)$ and $\sin s\alpha x \psi_r(y)$ respectively. Integrating over the channel height, h, and streamwise wavelength of the fundamental harmonic, $2\pi/\alpha$, gives a system of non-linear, ordinary differential equations in time for the unknown functions, A_{mv} and B_{mv}. These have the form

$$\left.\begin{aligned}
\sum_m D1^v_{mr} \frac{dA_{mv}}{dt} &= \sum_m -A_{mv} D2^v_{mr} - B_{mv} D3^v_{mr} + \sum_u \sum_s \sum_m \sum_n [CAB^{vsu}_{rmn} A_{ms} B_{nu} \\
&\qquad + CBA^{vsu}_{rmn} B_{ms} A_{nu}], \\
\sum_m D1^v_{mr} \frac{dB_{mv}}{dt} &= \sum_m -B_{mv} D2^v_{mr} + A_{mv} D3^v_{mr} + \sum_u \sum_s \sum_m \sum_n [CAA^{vsu}_{rmn} A_{ms} A_{nu} \\
&\qquad + CBB^{vsu}_{rmn} B_{ms} B_{nu}] \quad (r = 1, 2, \ldots, \quad v = 0, 1, 2, \ldots).
\end{aligned}\right\} \tag{2.8}$$

The various coefficients are given in the appendix. Equations (2.8) are solved by numerical integration in time. Initial conditions must be specified of course; however, in the present physical context it is the long time solution which is of interest and hence the precise nature of the initial conditions is not crucial. More will be said of this later.

3. Some analytical results

3.1. *Linear theory*

From elementary considerations we may divide the equations of motion into symmetric and antisymmetric y modes. It will be desirable to introduce the following nomenclature: 1, 3, 5, 7, ... are antisymmetric or odd modes; 2, 4, 6, 8, ... are symmetric or even modes. Note that the odd modes are antisymmetric in the velocity, $\partial\psi/\partial y$, but symmetric in ψ and $\partial\psi/\partial x$, see (2.6) and (2.7). Similarly the even modes are symmetric in $\partial\psi/\partial y$ but antisymmetric in ψ and $\partial\psi/\partial x$. Hence the symmetry or antisymmetry is with respect to velocity, not stream function. It will be important to keep this distinction in mind. Further, as is well known, it is an odd mode which is unstable in the linear theory, not an even one as might be expected intuitively.

Again, from elementary considerations each harmonic, 0, α, 2α, etc., is independent in the linear theory. Indeed one of the goals of linear theory is to determine the harmonic which gives the smallest Reynolds number at which the flow is unstable.

Finally in this section we attempt to further motivate the choice of functions, $\psi_m(y)$. We shall show that the functions selected are closely related to the eigenfunctions for $\alpha \equiv 0$. For $\alpha \equiv 0$ or equivalently, $\partial/\partial x \equiv 0$, and a linear analysis, (2.1) may be reduced to

$$\frac{1}{R}\frac{\partial^4\psi}{\partial y^4} - \frac{\partial}{\partial t}\left(\frac{\partial^2\psi}{\partial y^2}\right) = 0. \tag{3.1}$$

Assuming a solution of the form

$$\psi(y,t) = e^{St}\hat{\psi}(y), \tag{3.2}$$

we have an eigenvalue problem of the form

$$\frac{1}{R}\frac{d^4\hat{\psi}}{dy^4} - s\frac{d^2\hat{\psi}}{dy^2} = 0, \tag{3.3}$$

where s is the eigenvalue. Equation (3.3) is readily solved subject to the boundary conditions (2.5) and the eigenvalues and eigenfunctions obtained. They are

$$S_{2m} = -\frac{(2\pi)^2}{R}, -\frac{(4\pi)^2}{R}, \ldots, -\frac{(2m\pi)^2}{R}, \quad m = 1, \ldots, \tag{3.4}$$

where the eigenfunction is

$$\hat{\psi}_{2m} = 1 - \cos 2m\pi y \tag{3.5}$$

and

$$S_{(2m-1)} \approx -\frac{(3\pi)^2}{R}, \ldots, -\frac{(2m-1)^2\pi^2}{R}, \quad m = 2, \ldots, \tag{3.6}$$

where

$$\psi_{(2m-1)} \approx 1 - \cos(2m-1)\pi y; \tag{3.7}$$

(3.6) and (3.7) are approximate. The exact eigenvalues satisfy the transcendental equation

$$(-S_m R)^{\frac{1}{2}} \sin(-S_m R)^{\frac{1}{2}} + 2\cos(-S_m R)^{\frac{1}{2}} = 2, \tag{3.8}$$

with the eigenfunction satisfying

$$\psi_m = \left\{\frac{1-\cos\lambda_m}{\sin\lambda_m - \lambda_m}\sin\lambda_m y + \cos\lambda_m y - \frac{\lambda_m[1-\cos\lambda_m]}{\sin\lambda_m - \lambda_m}y - 1\right\},$$

where

$$\lambda_m \equiv (-S_m R)^{\frac{1}{2}}.$$

Note that (3.4) and (3.5) satisfy (3.8) and (3.9) exactly. The similarity of the eigenfunctions (3.5), (3.7) and (3.9) to our somewhat simpler modes of (2.7) is apparent. Note that for $\alpha = 0$ the eigenvalues, S_m, are all real and negative for all R and hence represent monotonically decaying motion with no oscillations. Of course, they all approach zero as R approaches infinity.

3.2. *Non-linear theory*

In the non-linear theory, in general, the symmetric and antisymmetric y modes are coupled and all streamwise harmonics are coupled. However, certain special analytical properties still hold which lend insight into the physical process and these will be discussed here.

First of all, with regard to the y modes, we shall show the following. (i) If only odd modes are retained in the analysis, the non-linear terms are identically zero. Recall that unstable modes are odd according to the linear theory. (ii) If both even and odd modes are retained, the (unstable) odd modes will parametrically excite the even modes even if the initial conditions on the even modes are identically zero. (iii) However, if the initial conditions on the odd modes are identically zero, they will never be excited. (iv) There will be non-linear coupling among the even modes, even if no odd modes are retained. From the above it is clear that even and odd modes have a basically different character in the non-linear theory.

Note that, if E and F or $G1$, $G2$, $G3$ are zero, then, from the formulae given in the appendix, CAB, CBA, CAA, CBA are zero and hence non-linear terms vanish from (2.8). For brevity the subscripts are omitted here.

Thus in order to prove the above statements it is sufficient to demonstrate that the coefficients, $G1_{ijk}$ etc. (see appendix) have the following properties.

If i and j are even, then: (*a*) k odd implies $G1_{ijk}$ etc. are zero; (*b*) k even implies $G1_{ijk}$ etc. are not zero. If i and j are odd, then: (*c*) k odd implies $G1_{ijk}$ etc. are zero; (*d*) k even implies $G1_{ijk}$ etc. are not zero. Therefore (i) follows from (c), (ii) follows from (*d*), (iii) follows from (*a*) and (c), (iv) follows from (*b*).

The properties (*a*), (*b*), (*c*), (*d*) may be verified by examining the definitions of $G1_{ijk}$ etc. in the appendix and considering the symmetry and antisymmetry of the modal functions, $\psi_m(y)$, and their derivatives.

Secondly, with regard to the streamwise harmonics, there is no non-linear coupling if only a single harmonic, α, is retained. Hence a minimum of two harmonics is required to obtain a non-trivial non-linear effect. In order to show this one need only demonstrate that $E_{111} = F_{111} = 0$. This is readily done using the formulae of the appendix.

4. Numerical results

4.1. *Linear theory*

A series of calculations was made with the non-linear terms deleted to verify that the proposed method could reproduce the known results for the linear problem. Thomas's (1953) results will be taken as a standard by which the present method may be assessed. The numerical results are obtained in the form of time histories of the functions, A_{mn} and B_{mn}. A typical result for A_{11} is shown in figure 2. For this example the flow is unstable and a slowly increasing exponential, oscillatory growth is observed after the initial transient has been passed, i.e. roughly for $t > 50$. From such time histories the growth rate, S_R, and frequency, S_I, may be determined by fitting the time history with a normalized curve

$$e^{-S_R t}\sin S_I t.$$

This will permit us to determine the eigenvalue of the most amplified mode, S_R, S_I. Since in the linear theory the even and odd modes are decoupled, this may be done for both symmetric and antisymmetric modes. These complex eigenvalues, S_R and S_I, may be compared with those of Thomas (also one could compare with the results of Lin (1955), but these are less accurate).

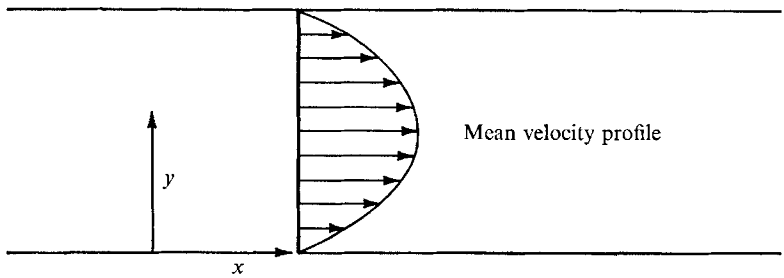

FIGURE 1. Geometry of plane Poiseuille flow.

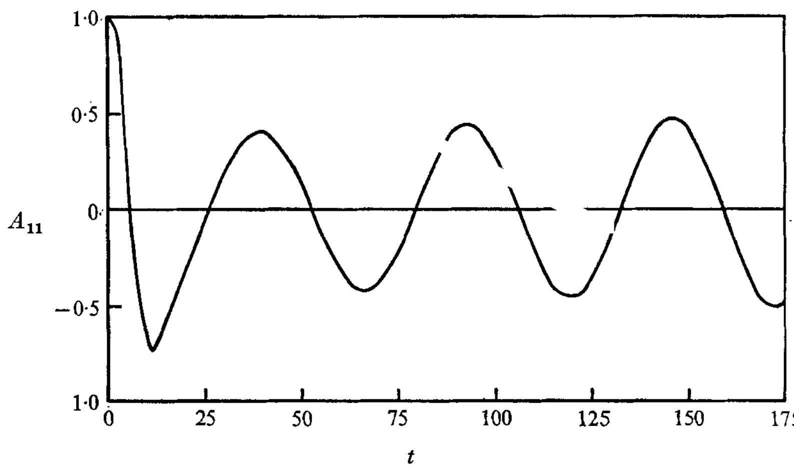

FIGURE 2. Time history of first mode, first harmonic. $R = 80{,}000$, $\alpha = 2$, $M = 48$, $N = 1$.

An important question in the use of the Galerkin method is the number of modes required for convergence. In figures 3 and 4, S_R and S_I are plotted *vs.* the number of y modes. Also shown are Thomas's (1953) results for the first odd mode using 100 finite-difference points. As may be seen, approximately 40 modes are required for good convergence. A 48-mode solution requires approximately 5 min on an IBM 360–67 computer.

In figures 5 and 6 results are presented for S_R and S_I for a range of Reynolds number and $\alpha = 2$. Twenty-odd modes (equivalent to 40 in figures 3 and 4) were used. Again the results agree very well with those of Thomas. Finally, in figures 7 and 8 similar results for a range of α and $R = 80{,}000$ are given.

It is important to remark that, for larger R and α, more modes are required for convergence and conversely for smaller R and α fewer modes are needed. For example, when $R = 20{,}000$ only half as many modes are required as for

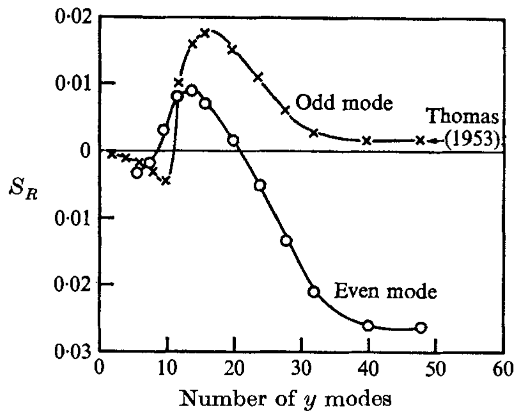

FIGURE 3. Convergence study. $\alpha = 2$, $R = 80{,}000$.

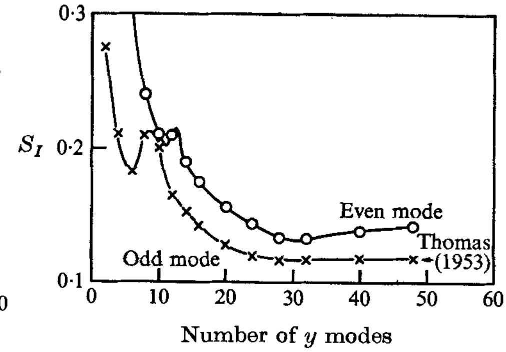

FIGURE 4. Convergence study. $\alpha = 2$, $R = 80{,}000$.

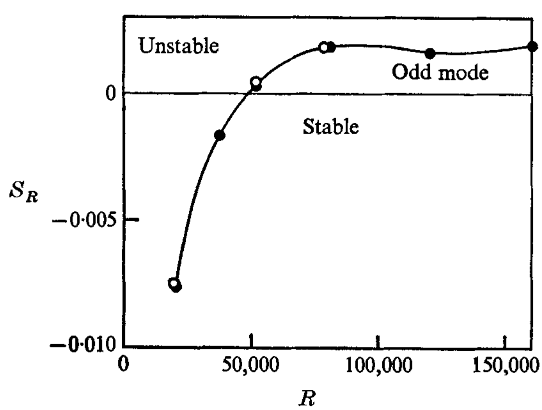

FIGURE 5. Growth rate *vs.* Reynolds number. $\alpha = 2$. ●, Dowell (20 modes); ○, Thomas (50 points).

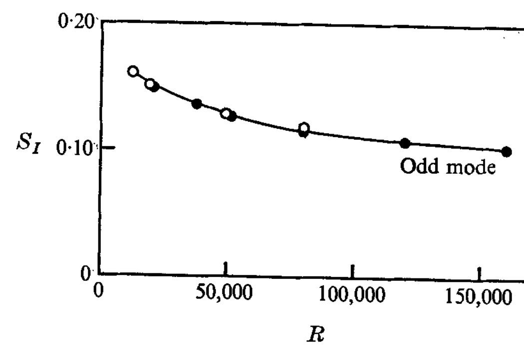

FIGURE 6. Frequency *vs.* Reynolds number. $\alpha = 2$. ●, Dowell (20 modes); ○, Thomas (50 points).

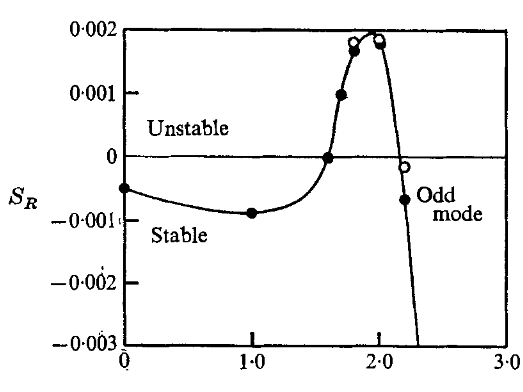

FIGURE 7. Growth rate *vs.* wave-number. $R = 80{,}000$. ●, Dowell (20 modes); ○, Thomas (50 points).

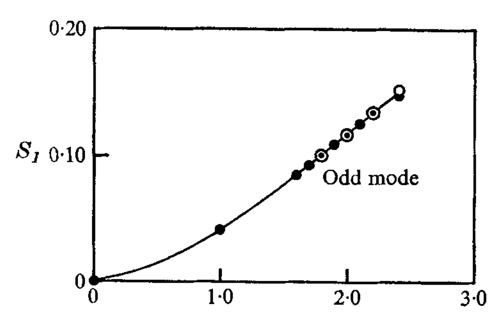

FIGURE 8. Frequency *vs.* wave-number. $R = 80{,}000$. ●, Dowell (20 modes); ○, Thomas (50 points).

$R = 80{,}000$, and, of course, for $\alpha = 0$ only one mode is needed, see §3. Unfortunately the flow is stable for $R = 20{,}000$ and/or $\alpha = 0$.

It is clear that the method can be used to obtain the results of linear theory in a satisfactory manner.

4.2. *Non-linear theory*

When the non-linear terms are retained, the exponential growth of an unstable flow does not continue indefinitely, but instead the flow reaches asymptotically some finite amplitude determined by a balance between the linear and non-linear terms.

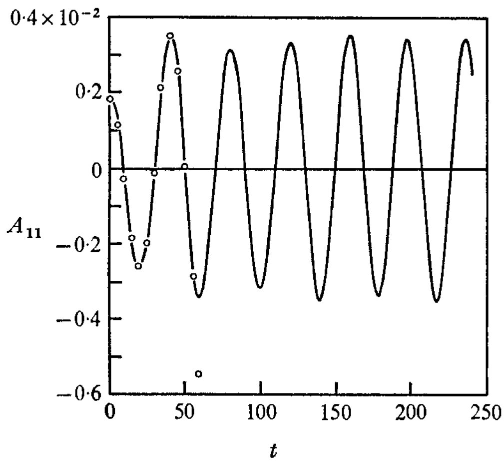

FIGURE 9. Time history of first mode, first harmonic. $N = 1$, $M = 16$, $R = 80{,}000$, $\alpha = 2$. ——, non-linear; ○, linear.

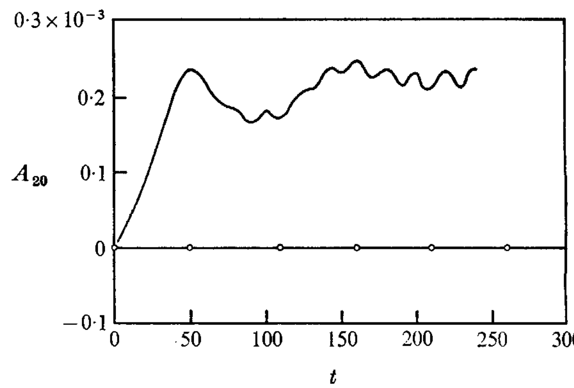

FIGURE 10. Time history of second mode, zeroth harmonic. $N = 1$, $M = 16$, $R = 80{,}000$, $\alpha = 2$. ——, non-linear; ○, linear.

One may estimate the limit cycle amplitude from an order-of-magnitude analysis which equates the linear and non-linear terms of (2.1) or (2.8). The result is

$$\psi \sim A \sim 2\pi^3/R, \tag{4.1}$$

for $R = 80{,}000$, $\psi \sim 10^{-3}$. This rough estimate was used to select initial conditions which would be near the final limit cycle so that the initial transient would be as short as possible.

After a few preliminary runs it became clear that it would not be practical to retain a sufficient number of modes to ensure convergence. Thus the calculations reported here for the non-linear problem are of a qualitative character. A Reynolds number of $R = 80{,}000$ and wave-number of $\alpha = 2$ were chosen. Sixteen y modes and two harmonics, $v = 0$ and 1, were retained, for a total of 32 degrees of freedom. Results for two modal functions, A_{11} and A_{20}, are given in figures 9 and 10. We also indicate the results from linear theory *for the same initial conditions*. The results are quite different. The linear theory would give $A_{20} = 0$ and A_{11} an exponentially increasing oscillation. The non-linear theory shows that A_{20} is excited by non-linear coupling and A_{11} has a constant amplitude, oscillatory behaviour due to non-linear stabilization. It is interesting to note that the amplitude of A_{21} (not shown) is approximately 5×10^{-4} and that of A_{10} approximately $0{\cdot}1 \times 10^{-4}$. Hence the primary response is in the odd, first harmonic and even zeroth harmonic. Note the difference in time dependence

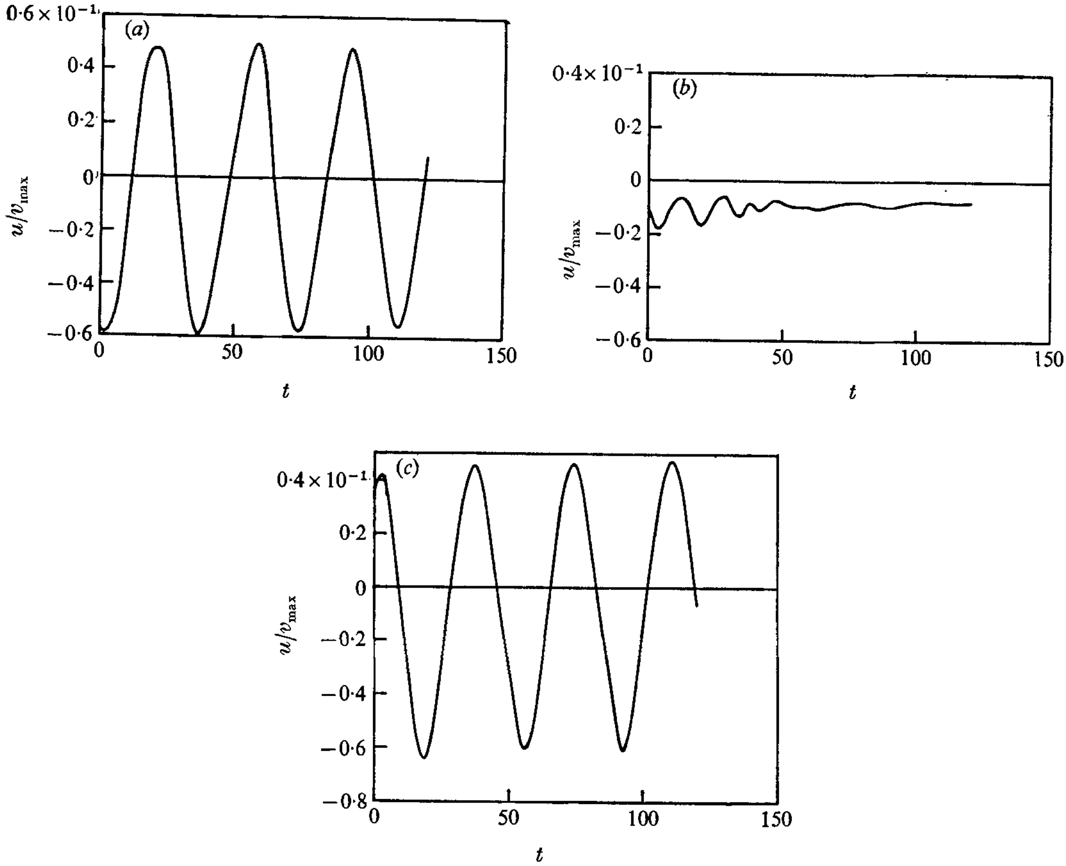

FIGURE 11. (*a*) Velocity time history; $R = 80{,}000$, $\alpha = 2$, $M = 16$, $N = 1$, $y = 0{\cdot}75$; (*b*) velocity time history; $R = 80{,}000$, $\alpha = 2$, $M = 16$, $N = 1$, $y = 0{\cdot}5$; (*c*) velocity time history; $R = 80{,}000$, $\alpha = 2$, $M = 16$, $N = 1$, $y = 0{\cdot}25$.

of these dominant modes. A_{20} is nearly constant with time while A_{11} is sinusoidal. Hence the change in the mean flow will be a symmetrical one while the fluctuating changes will be antisymmetrical.

To put the results in somewhat more physical terms we show the time histories of the streamwise velocity for various positions across the channel in figure 11 (*a*)–(*c*). Here the perturbation velocity, u, is non-dimensionalized by the mid-channel mean velocity, $V_{max} = \frac{1}{4}V$. One may see from these results that the mean flow profile will be somewhat symmetrically blunted from its original stable (laminar) profile. However, the quantitative effect is small. Presumably it would increase as the Reynolds number increases. Note again the oscillatory part of the velocity perturbation is antisymmetric.

Although the number of modes is too small for quantitative accuracy, it is thought the results are qualitatively significant; in particular (i) the parametric excitation of even modes by odd modes, (ii) the steady behaviour of even modes and oscillatory behaviour of odd ones are thought to be intrinsic to the problem whatever the number of modes.

From results using various (smaller) modal combinations it is thought that the quantitative effect of additional modes will be to reduce the over-all amplitude of the response.

The results reported here took approximately 2 h on an IBM 360–67 computer.

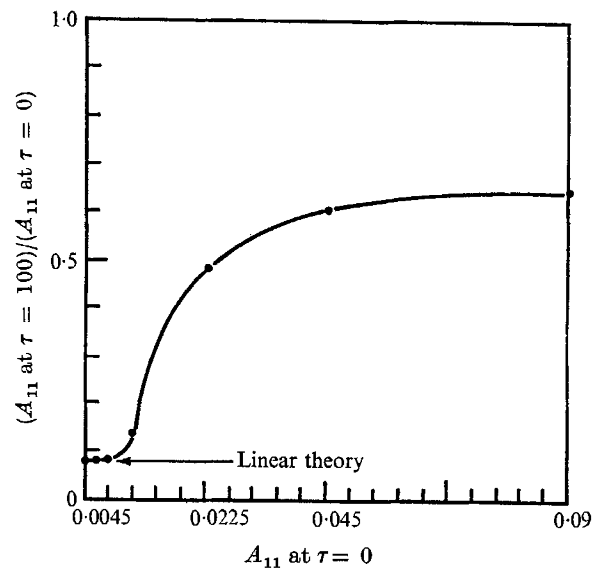

FIGURE 12. Amplitude ratio *vs.* initial amplitude. $R = 8000$, $\alpha = 1$, $M_{max} = 8$.

Finally a brief study was made to see whether a large initial disturbance destabilizes a flow which is stable with respect to small (infinitesimal) disturbances. According to the linear theory the flow is stable for $\alpha = 1$ and $R = 8000$. An investigation of decay *vs.* initial amplitude gave the results shown in figure 12. The ratio of amplitude at the initial instant, A_{11} at $\tau = 0$, is used to normalize the amplitude one cycle later, A_{11} at $\tau = 100$. Although in all cases the oscillation decays, the decay is less—i.e. the amplitude ratio is larger—as the initial amplitude increases. For large initial amplitude, the amplitude ratio appears to approach an asymptote which is less than one. Incidentally there is very little change in the frequency of oscillation with initial amplitude. Also eight modes give sufficient convergence for this α and R.

Hence it may be concluded that in this particular case the flow remains stable for large initial amplitudes but is less so than for small ones. It should be noted that Meksyn & Stuart (1951) have concluded that for some R and α the flow may be destabilized by large initial disturbances.

In general one should not expect the limit cycle to be unique and it is of interest to examine a variety of initial conditions. We hope to do this in future work and also to extend the solutions to larger numbers of modes. The initial conditions chosen were on the basis of a gross estimate of the amplitude from order-of-magnitude considerations and the distribution of modal amplitudes was chosen on the basis of linear theory results.

The numerical integration technique used was one of the standard finite-difference formulae. The only precaution taken was to require that the time increment was sufficiently small to ensure numerical stability for the highest-frequency (shortest period) mode. In practice this imposes no essential restriction as the time interval necessary to ensure good definition of the oscillations is shorter than this. A typical time interval was $\Delta\tau = 0{\cdot}2 \rightarrow 1{\cdot}0$.

5. Conclusions

From the results obtained here it is clear that the treatment of non-linear limit cycle oscillations of viscous flows is feasible. However, computations for a practical range of parameters will require advances in computer technology of perhaps a factor of 10 in computation speed. There is a possibility of reducing the amount of computation required by combining Galerkin's method with an eigenfunction expansion. One could first use the Galerkin method for the *linear* problem to compute the eigenfunctions in terms of the primitive modes for arbitrary R and α. Then the non-linear problem could be treated by an expansion in terms of these eigenfunctions which would presumably reduce the number of modes required for the non-linear problem. That is, an expansion in terms of eigenfunctions would be more rapidly convergent than the one used here in terms of primitive modes. This possibility remains to be investigated.

Among the interesting qualitative features shown to date for plane Poiseuille flow are: (i) the parametric excitation of even modes (stable in the linear theory) by odd modes (unstable in the linear theory); (ii) the steady time dependence of even modes contrasted with the oscillatory behaviour of odd modes.

A brief study was made to investigate whether, for small Reynolds number where linear theory predicts a stable flow, the flow may be made unstable by a sufficiently large initial disturbance. A preliminary investigation of this possibility gave negative results. That is, while the decay was decreased with larger initial disturbances, the flow was stable with respect to large disturbances if it was stable with respect to small ones.

Finally, a word may be said about three-dimensional effects. Three-dimensionality offers no problem in terms of formulation (or computation for the *linear* theory). However, for the non-linear theory, three-dimensional computations would not appear to be feasible at present. Hence the present work was restricted to the two-dimensional case.

This work was supported by NASA grants NGR 31-001-059 and NGR 31-001-146.

Appendix

$$D1^v_{mr} \equiv (v\alpha)^2 C3_{mr} - C2_{mr},$$

$$D2^v_{mr} \equiv \frac{C1_{mr} - 2(v\alpha)^2 C2_{mr} + (v\alpha)^4 C3_{mr}}{R},$$

$$D3^v_{mr} \equiv (v\alpha)^3 C4_{mr} - (v\alpha) C5_{mr} - 2(v\alpha) C3_{mr},$$

where

$$C1_{mr} \equiv \int_0^1 \psi_m^{\mathrm{iv}} \psi_r \, dy = (m-1)^4 \pi^4 [H_{(m-1)(r-1)} - H_{(m-1)(r+1)}] - (m+1)^4 \pi^4 [H_{(m+1)(r-1)} - H_{(m+1)(r+1)}],$$

$$C2_{mr} \equiv \int_0^1 \psi_m'' \psi_r \, dy = -(m-1)^2 \pi^2 [H_{(m-1)(r-1)} - H_{(m-1)(r+1)}] + (m+1)^2 \pi^2 [H_{(m+1)(r-1)} - H_{(m+1)(r+1)}],$$

$$C3_{mr} \equiv \int_0^1 \psi_m \psi_r \, dy = H_{(m-1)(r-1)} - H_{(m-1)(r+1)} - H_{(m+1)(r-1)} - H_{(m+1)(r+1)},$$

where the prime denotes d/dy and

$$\begin{aligned} H_{ij} &\equiv \int_0^1 \cos i\pi y \cos j\pi y \, dy \\ &= 1 \quad \text{for} \quad i = j = 0, \\ &= \tfrac{1}{2} \quad \text{for} \quad i = \pm j \neq 0, \\ &= 0 \quad \text{for} \quad i \neq \pm j. \end{aligned}$$

$$\begin{aligned} C4_{mr} &\equiv \int_0^1 y \psi_m \psi_r \, dy - \int_0^1 y^2 \psi_m \psi_r \, dy \\ &= \{J_{(m-1)(r-1)} - J_{(m+1)(r-1)} - J_{(m-1)(r+1)} + J_{(m+1)(r+1)}\} \\ &\quad - \{J2_{(m-1)(r-1)} - J2_{(m+1)(r-1)} - J2_{(m-1)(r+1)} + J2_{(m+1)(r+1)}\}, \end{aligned}$$

$$\begin{aligned} C5_{mr} &\equiv \int_0^1 y \psi_m'' \psi_r \, dy - \int_0^1 y^2 \psi_m'' \psi_r \, dy \\ &= \{-(m-1)^2 \pi^2 [J_{(m-1)(r-1)} - J_{(m-1)(r+1)}] \\ &\quad + (m+1)^2 \pi^2 [J_{(m+1)(r-1)} - J_{(m+1)(r+1)}]\} \\ &\quad - \{-(m-1)^2 \pi^2 [J2_{(m-1)(r-1)} - J2_{(m-1)(r+1)}] \\ &\quad + (m+1)^2 \pi^2 [J2_{(m+1)(r-1)} - J2_{(m+1)(r+1)}]\}, \end{aligned}$$

where

$$J_{ij} \equiv \int_0^1 y \cos i\pi y \cos j\pi y \, dy = \tfrac{1}{2}[I_{(i+j)} + I_{(i-j)}],$$

$$I_k \equiv \int_0^1 y \cos k\pi y \, dy = \begin{cases} [(-1)^k - 1]/(k\pi)^2 & \text{for} \quad k \neq 0, \\ \tfrac{1}{2} & \text{for} \quad k = 0, \end{cases}$$

$$J2_{ij} \equiv \int_0^1 y^2 \cos i\pi y \cos j\pi y \, dy = \tfrac{1}{2}[I2_{(i+j)} + I2_{(i-j)}],$$

$$I2_k \equiv \int_0^1 y^2 \cos k\pi y \, dy = \begin{cases} 2(-1)^k/(k\pi)^2 & \text{for} \quad k \neq 0, \\ \tfrac{1}{3} & \text{for} \quad k = 0. \end{cases}$$

$$CAB^{vsu}_{rmn} \equiv E_{suv}[-(u\alpha)^3 G1_{mnr} + (u\alpha) G2_{nmr}] + F_{suv}[-(u\alpha)^2 G1_{nmr} + G3_{nmr}](s\alpha),$$

$$CBA^{vsu}_{rmn} \equiv F_{suv}[(u\alpha)^3 G1_{mnr} - (u\alpha) G2_{nmr}] - E_{suv}[-(u\alpha)^2 G1_{nmr} + G3_{nmr}](s\alpha),$$

$$CAA^{vsu}_{rmn} \equiv F_{uvs}[(u\alpha)^3 G1_{mnr} - (u\alpha) G2_{nmr}] + F_{svu}[-(u\alpha)^2 G1_{nmr} + G3_{nmr}](s\alpha),$$

$$CBB^{vsu}_{rmn} \equiv F_{svu}[-(u\alpha)^3 G1_{mnr} + (u\alpha) G2_{nmr}] - F_{uvs}[-(u\alpha)^2 G1_{nmr} + G3_{nmr}](s\alpha),$$

where

$$E_{ijk} \equiv \tfrac{1}{2}[\mathscr{B}_{(i+j+k)} + \mathscr{B}_{(i+j-k)} + \mathscr{B}_{(i-j+k)} + \mathscr{B}_{(i-j-k)}],$$

$$F_{ijk} \equiv \tfrac{1}{2}[\mathscr{B}_{(i-j+k)} + \mathscr{B}_{(k-i+j)} - \mathscr{B}_{(k+i+j)} - \mathscr{B}_{(k-i-j)}],$$

and

$$\mathscr{B}_i \equiv 1 \quad \text{for} \quad i = 0,$$
$$\equiv 0 \quad \text{for} \quad i \neq 0.$$

$$G1_{ijk} \equiv \int_0^1 \psi_i' \psi_j \psi_k \, dy = \tfrac{1}{2}(i-1)[K_{(i-1)(j+k-2)} + 2K_{(i-1)(j-k)} - 2K_{(i-1)(j+k)} - K_{(i-1)(j-k-2)} - K_{(i-1)(j-k+2)} + K_{(i-1)(j+k+2)}] + \tfrac{1}{2}(i+1)\pi[K_{(i+1)(j+k-2)} + 2K_{(i+1)(j-k)} - 2K_{(i+1)(j+k)} - K_{(i+1)(j-k+2)} - K_{(i+1)(j-k+2)} + K_{(i+1)(j+k+2)}],$$

$$G2_{ijk} \equiv \int_0^1 \psi_i'' \psi_j' \psi_k \, dy$$
$$= (i-1)^2\pi^2\{\tfrac{1}{2}(j-1)\pi[K_{(j-1)(i+k-2)} + K_{(j-1)(i-k)} - K_{(j-1)(i+k)} - K_{(j-1)(i-k-2)}] + \tfrac{1}{2}(j+1)\pi[-K_{(j+1)(i+k-2)} - K_{(j+1)(i-k)} + K_{(j+1)(i+k)} + K_{(j+1)(i-k-2)}]\} + (i+1)^2\pi^2\{\tfrac{1}{2}(j-1)\pi[-K_{(j-1)(i+k)} - K_{(j-1)(i-k+2)} + K_{(j-1)(i+k+2)} + K_{(j-1)(i-k)}] + \tfrac{1}{2}(j+1)\pi[K_{(j+1)(i+k)} + K_{(j+1)(i-k+2)} - K_{(j+1)(i+k+2)} - K_{(j+1)(i-k)}]\},$$

$$G3_{ijk} \equiv \int_0^1 \psi_i''' \psi_j \psi_k \, dy = \tfrac{1}{2}(i-1)^3\pi^3\{K_{(i-1)(j+k-2)} + 2K_{(i-1)(j-k)} - 2K_{(i-1)(j+k)} - K_{(i-1)(j-k-2)} - K_{(i-1)(j-k+2)} + K_{(i-1)(j+k+2)}\} - \tfrac{1}{2}(i+1)^3\pi^3\{K_{(i+1)(j+k-2)} + 2K_{(i+1)(j-k)} - 2K_{(i+1)(j+k)} - K_{(i+1)(j-k-2)} - K_{(i+1)(j-k+2)} + K_{(i+1)(j+k+2)}\},$$

where

$$K_{ij} \equiv \int_0^1 \sin i\pi y \cos j\pi y \, dy$$
$$= [i/(i^2-j^2)][1-(-1)^{i+j}]/\pi \quad \text{for} \quad i \neq \pm j,$$
$$= 0 \quad \text{for} \quad i = \pm j.$$

REFERENCES

Dixon, T. N. & Hellums, J. D. 1967 A study on stability and incipient turbulence in Poiseuille and plane-Poiseuille flow by numerical finite difference simulation. *A.I.Ch.E.* **13**, 866–872.

Dolph, C. L. & Lewis, D. C. 1958 On the application of infinite systems of ordinary differential equations to perturbations of plane Poiseuille flow. *Q. Appl. Math.* **16**, 97–110.

Eckhaus, W. 1965 *Studies in Nonlinear Stability Theory*. New York: Springer Verlag.

Gallagher, A. P. & Mercer, A. McD. 1962 On the behaviour of small disturbances in plane Couette flow. *J. Fluid Mech.* **13**, 91–100.

Grosch, C. E. & Salwan, H. 1968 The stability of steady and time-dependent plane Poiseuille flow. *J. Fluid Mech.* **34**, 177–205.

Lin, C. C. 1955 *The Theory of Hydrodynamic Stability*. Cambridge University Press.

Meksyn, D. & Stuart, J. T. 1951 Stability of viscous motion between parallel flows for finite disturbances. *Proc. Roy. Soc.* A **208**, 517–526.

Stuart, J. T. 1960 On the nonlinear mechanics of wave disturbances in stable and unstable parallel flows. 1. The basic behaviour in plane Poiseuille flow. *J. Fluid Mech.* **9**, 357–370.

Thomas, L. H. 1953 The stability of plane Poiseuille flow. *Phys. Rev.* **91**, 780–783.

Watson, J. 1960 On the nonlinear mechanics of wave disturbances in stable and unstable parallel flow. 2. The development of a solution for plane Poiseuille flow and for plane Couette flow. *J. Fluid Mech.* **9**, 371–389.

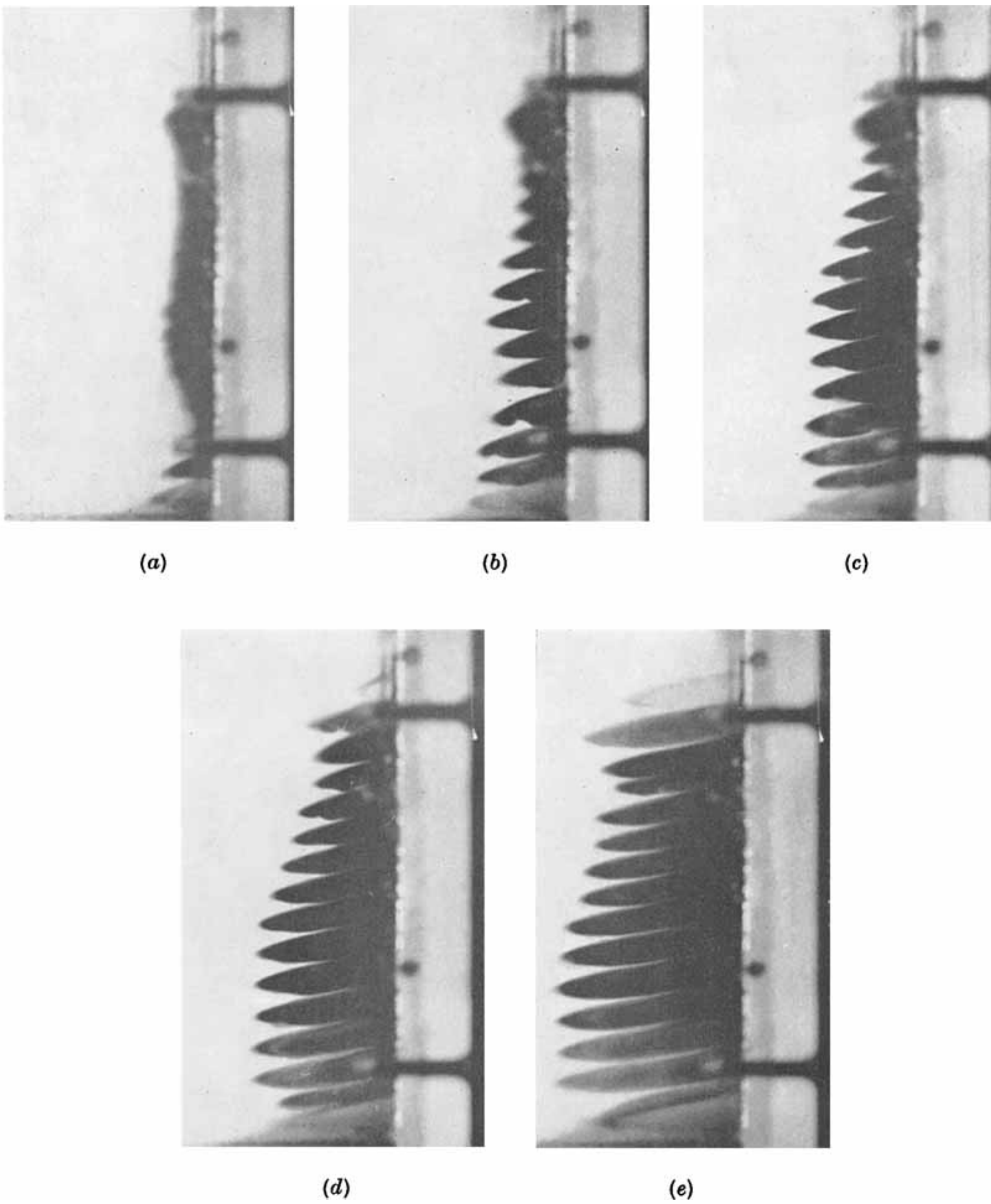

FIGURE 1. The development of layers in a stratified brine solution subject to heating through a vertical side-wall. The screws, seen as distinct horizontal bars in the vertical Perspex wall, are 5 cm apart. The initial density gradient in the brine is 8×10^{-4} g cm^{-4}. The photographs were taken at the following times after a 100 watt light was first switched on 23 cm from the side wall: (*a*) 16 min, (*b*) 19·5 min, (*c*) 21·75 min, (*d*) 24 min, (*e*) 28·25 min.

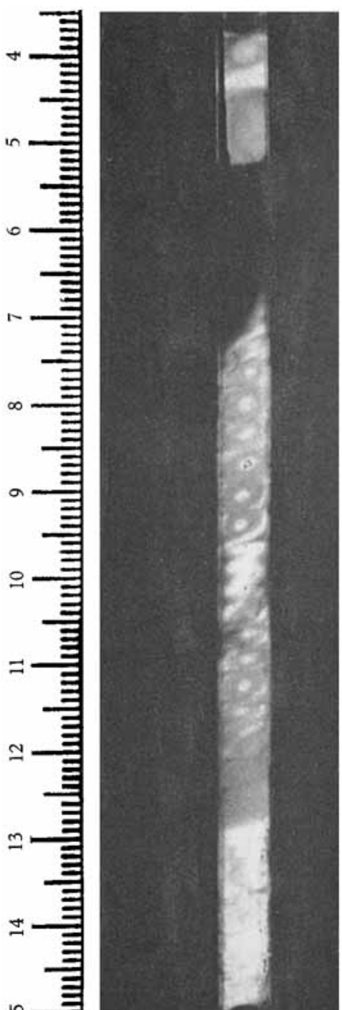

FIGURE 8. The cells formed at the onset of instability in the slot experiments. The initial density gradient due to salinity is $4{\cdot}46 \times 10^{-3}$ g cm^{-4} and the temperature difference across the slot is 4·2 °C. The hot bath is to the right and the cold bath to the left. The scale is in cm.

FIGURE 11. Photograph showing the layers developed right across the tank in the experiment described in section 4. The dye indicates the motions in the layers.